Comprehensive Understanding of Structure-Controlling Factors of a Zinc Tetraphenylporphyrin Thin Film Using pMAIRS and GIXD Technique

Miyako Hada,[a] Nobutaka Shioya,[a] Takafumi Shimoaka,[a] Kazuo Eda,[b] Masahiko Hada,[c] and Takeshi Hasegawa*[a]

Abstract: The performance of an organic electronic device is significantly influenced by the anisotropic molecular structure in the film, which has long been difficult to predict especially for a solution process. In the present study, a zinc tetraphenylporphyrin (ZnTPP) thin film prepared by a solution process is chosen to comprehensively explore the molecular arrangement mechanism as a function of representative film-preparation parameters: solvent, film-preparation technique, and thermal annealing. The anisotropic structure is first analyzed by using the combination technique of infrared p-polarized multiple-angle incidence resolution spectrometry (pMAIRS) and grazing incidence X-ray diffraction (GIXD), which readily reveal the molecular orientation and crystal structure, respectively. As a result, the real dominant factor is found to be the 'evaporation time of the solvent,' which determines the initial two different molecular arrangements, types-I and -II, while the thermal annealing is found to play an additional role of improving the molecular order. The correlation between the molecular orientation and the crystal structure has also been revealed through the individual orientation analysis of the porphyrin and phenyl rings.

Introduction

Organic semiconductors used for thin film electronic devices are made of polymeric or small-molecular materials. Most of the polymeric semiconductors represented by poly-(3-hexylthiophene-2,5-diyl) (P3HT) and poly[2-methoxy- 5-(2-ethylhexyloxy)-1,4-phenylenevinylene] (MEH-PPV) are highly soluble in an organic solvent, and thus a thin film can be prepared easily and inexpensively via a solution process such as the spin-coating[1,2] and inkjet printing[3-5] techniques. The polymeric materials, however, have an intrinsic issue of a low charge mobility[6] due to a poor molecular ordering in the thin film.

In contrast, small-molecular materials represented by pentacene and dinaphtho[2,3-*b*:2'3'-*f*]thieno[3,2-*b*]thiophene (DNTT) exhibit high charge mobilities[7,8] thanks to a high crystallinity in the thin film. Unfortunately, however, these representative compounds have a low solubility in an organic solvent, which makes the film preparation difficult via a solution process. In fact, the vacuum vapor deposition[9] and molecular beam epitaxy[10-12] methods, which are unsuitable for a mass production, are thus often employed.

To overcome the dilemma, solvent-soluble small-molecular semiconductors accompanying additional chemical groups with a high affinity to organic solvents have been developed,[13-17] which are expected to possess both high solubility and high charge mobility. One of the materials is zinc tetraphenylporphyrin (ZnTPP; chart 1) that is composed of the porphyrin skeleton and four phenyl rings. By introducing the phenyl moieties, ZnTPP is made highly soluble in many organic solvents. Since porphyrin or phtalocyanine is a representative small-molecular organic semiconductor for electronic devices,[18] ZnTPP receives much attention as a promising compound and as a solution-processable small-molecular material for the devices.[19-22]

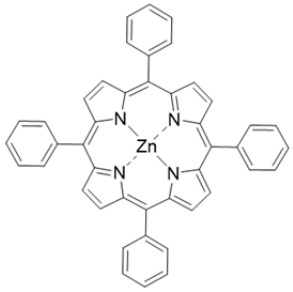

Chart 1. Chemical structure of zinc tetraphenylporphirin (ZnTPP)

The molecular orientation and crystal structure are key factors to discuss the thin film structure, both of which significantly influence the device performance. For example, a P3HT film is known to have some different molecular orientation, thiophenyl ring-parallel and ring-vertical orientations to the substrate surface,[23] in which the films exhibit largely different carrier mobility.[24,25] As well as P3HT, evaporated films of pentacene are also known to show different mobilities depending on the ring orientation and crystal structure.[26,27] Since the molecular structure in the thin film directly influences the device performance, both analysis and control of the molecular arrangement are of great importance.

Representative film-preparation parameters in a solution process to control the molecular arrangement in an organic thin film are "solvent"[28,29] and "film-preparation technique."[2] For instance, chloroform (Chl) and 1,2,4-trichlorobenzene (TCB), known as representative organic solvents exhibiting high and low volatile characters, respectively, yield largely different molecular arrangements.[28,29] In addition, the spin-coating (SC) technique makes the solvent evaporated quickly; while the solvent evaporates

[a] M. Hada, N. Shioya, Prof. T. Shimoaka, Prof. T. Hasegawa
Laboratory of Solution and Interface Chemistry, Division of Environmental Chemistry
Institute for Chemical Research, Kyoto University
Gokasho, Uji, Kyoto 611-0011, Japan
htakeshi@scl.kyoto-u.ac.jp
[b] Prof. K. Eda
Department of Chemistry, Graduate school of Science
Kobe University
1-1 Rokko-dai, Nada-ku, Kobe, Hyogo 657-8501, Japan
[c] Prof. M. Hada
Department of Chemistry, Division of Science and Engineering
Tokyo Metropolitan University
1-1 Minami-Osawa, Hachioji, Tokyo 192-0397, Japan

Supporting information for this article is given via a link at the end of the document.

slowly in a drop-casted (DC) film. Therefore, an appropriate combination of a solvent (Chl or TCB) and a film-preparation technique (SC or DC) controls the solvent "evaporation time," which finally controls the molecular arrangement in the film.

Another important film-preparation parameter is the "thermal annealing" technique, which is often used to order or convert the molecular arrangement in a thin film.[30,31] For example, the thermal annealing improves the semiconductor properties (i.e., charge mobility, on/off ratio, etc.) of an etioporphyrin-I thin film.[32]

In the present study, the film structure of a ZnTPP thin film is studied comprehensively and systematically for all the combinations of the three film-preparation parameters in terms of the molecular orientation and the crystal structure.

For the purpose, we have first employed the combined analytical technique of infrared p-polarized multiple-angle incidence resolution spectrometry (pMAIRS)[33-37] and the grazing incidence X-ray diffraction (GIXD)[38,39] technique. The combination technique is quite powerful to reveal the correlation between the molecular orientation and crystal structure in a thin film: the molecular orientation of each chemical group in the thin film is revealed quantitatively by using pMAIRS and GIXD provides the crystal structure (and/or crystallinity). As a result, the molecular arrangement in the ZnTPP film has been found to have a wide variety of the molecular orientation and crystal structure, which can readily been controlled by choosing an appropriate combination of only three film-preparation parameters.

Results and Discussion

Molecular orientation in a ZnTPP film prepared from a Chl solution: Figure 1 shows pMAIRS spectra of the ZnTPP thin films prepared from the Chl solution (denoted as "Chl films"). The red and blue lines are the in-plane (IP) and out-of-plane (OP) spectra, respectively. The spectra of a-d in Figure 1 correspond to the samples a-d listed in Table 1, respectively. The band assignments of the spectra of ZnTPP were made after a DFT calculation, and the results are summarized in Table S1 (Supporting Information). The C–H out-of-plane deformation vibration (γ(C–H)) band of an aromatic ring appears in the low wavenumber region of 900–650 cm^{-1}; while the C–H in-plane deformation vibration (δ(C–H)) band appears in 1600–950 cm^{-1}. The γ(C–H) and δ(C–H) modes have transition moments perpendicular and parallel to the aromatic ring plane, respectively. In particular, the γ(C–H) mode is fortunately highly localized on the ring with a strong absorption coefficient, which is quite useful for analyzing the molecular orientation of the ring.[23,29]

As found in the Chl-SC film (Figure 1a), the pMAIRS-IP and -OP spectra have comparable band intensities in all the regions, which straightforwardly indicates that ZnTPP in the film has a random orientation. After annealing this film (denoted as "Chl-SC-A film"; Figure 1b), the bands at 798 and 718 cm^{-1}, both of which are assigned to the γ(C–H) modes of 'porphyrin' ring ($\gamma(C–H)_{por}$; Figure 2a),[40-42] develop significantly in the OP spectrum.

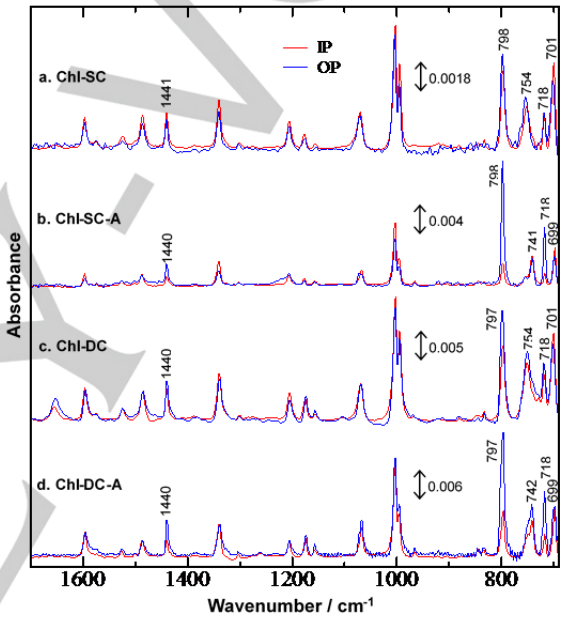

Figure 1. Infrared pMAIRS spectra of the ZnTPP thin films prepared from the Chl solution.

Table 1. The combination matrix of the three film-preparation parameters.

Sample	Solvent	Film-preparation technique	Annealing	Evaporation time
(a)	Chloroform (Chl)	Spin-Coating (SC)	×	Short
(b)	Chl	SC	Annealed	
(c)	Chl	Drop-Casting (DC)	×	
(d)	Chl	DC	Annealed	
(e)	1,2,4-trichlorobenzene (TCB)	SC	×	
(f)	TCB	SC	Annealed	
(g)	TCB	DC	×	Long
(h)	TCB	DC	Annealed	

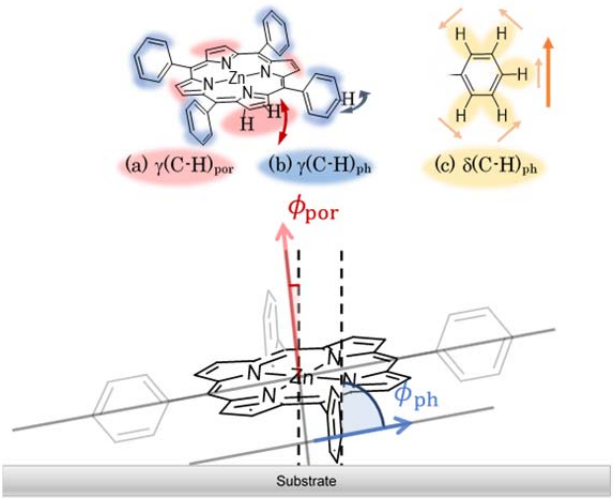

Figure 2. Schematic diagram of the vibration modes and the angles between the substrate surface normal and the direction of the transition moment: the angles of ϕ_{por} and ϕ_{ph} correspond to the $\gamma(C–H)_{por}$ (a) and $\gamma(C–H)_{ph}$ (b) modes, respectively.

Considering the surface selection rule of the pMAIRS spectra (see Experimental), the porphyrin ring should lie parallel to the substrate, that is, the face-on orientation.

The phenyl ring, on the other hand, is remained to have a random orientation as indicated by the intensity ratio of the γ(C–H) bands of the 'phenyl' ring ($\gamma(C–H)_{ph}$; Figure 2b)[40-42] at about 700 cm^{-1} between the IP and OP spectra. This trend is also found for the Chl-DC film (Figure 1c) and the annealed Chl-DC film ("Chl-DC-A film"; Figure 1b): the thermal annealing makes the molecular orientation improved for the porphyrin ring, while the phenyl ring is kept un-oriented (as summarized in Table 2).

Molecular orientation in a ZnTPP film prepared from a TCB solution: Figure 3 shows pMAIRS spectra of the ZnTPP thin films prepared from the 'TCB' solution (denoted as "TCB films"). The spectra in Figure 3e-3h correspond to the samples e-h listed in Table 1, respectively. Since TCB exhibits a low-volatile character (b.p. 214°C) in contrast to Chl (b.p. 59°C), a long evaporation time is needed for obtaining a TCB film. The lower evaporation rate than that of Chl significantly influences the molecular orientation in the generated film: all the TCB films have an extremely large dichroic ratio between the IP and OP spectra in a wide wavenumber range as shown in Figure 3. This indicates that the ZnTPP molecules have highly oriented structures irrespective of the thermal annealing. With a similar discussion to that of the spectra in Figures 1b and 1d, the porphyrin ring in all the TCB films takes the face-on orientation. Note that the $\gamma(C–H)_{por}$ bands at 798 and 718 cm^{-1} are shifted to 803 and 723 cm^{-1}, respectively, by changing the solvent from Chl to TCB. These band shifts will be discussed in detail later with related to XRD measurements.

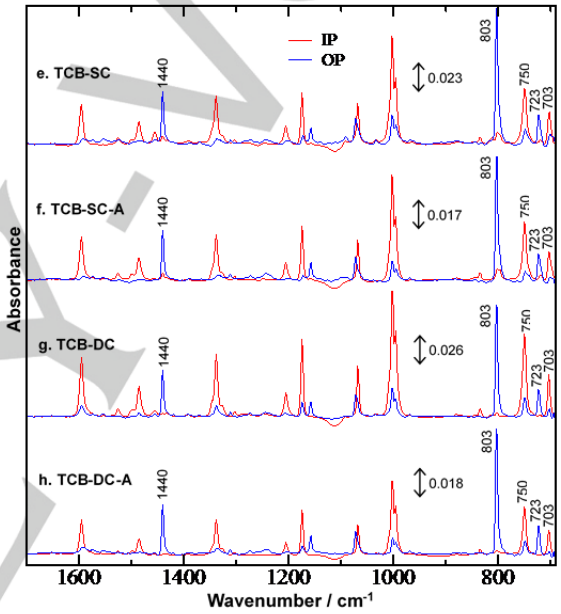

Figure 3. Infrared pMAIRS spectra of the ZnTPP thin films prepared from the TCB solution.

Table 2. The correlation between the crystal structure and the molecular orientation in the ZnTPP thin film as a function of the film-preparation parameter.

Film-preparation parameter	Molecular Orientation		Major molecular arrangement	Evaporation time
	Porphyrin ring	Phenyl ring		
Chl-SC	Random	Random	Amorphous (Type-I)	Short
Chl-SC-A	Face-on		Monoclinic (Type-I)	
Chl-DC	Random	Random	Amorphous (Type-I)	
Chl-DC-A	Face-on		Monoclinic (Type-I)	
TCB-SC	Face-on	Edge-on	Monoclinic (Type-II)	
TCB-SC-A				
TCB-DC	Face-on	Edge-on	Monoclinic (Type-II)	Long
TCB-DC-A				

The TCB films have another significant characteristic that even the $\gamma(C–H)_{ph}$ band exhibits an apparent MAIRS dichroism for the band at 703 cm^{-1}, i.e., the IP band is much stronger than the OP one. Therefore, in the TCB films, the phenyl ring is concluded to stand perpendicularly on the substrate (the edge-on orientation) in contrast to the orientation of the porphyrin ring.

Another notable band is the δ(C–H) band of the phenyl ring ($\delta(C–H)_{ph}$) at 1440 cm^{-1} appears dominantly in the OP spectrum. According to the DFT calculation, the transition moment of this band is parallel to the phenyl ring plane, and at the same time it is vertical to the phenyl-porphyrin bond, as shown in Figure 2c. In this manner, the TCB films have been found to have the phenyl ring with the edge-on orientation. In other words, the phenyl rings, which intrinsically have a rotational flexibility, are highly fixed in the TCB films. The highly oriented structure is thus found to be induced not by annealing, but by the slow-evaporation character of TCB (Table 2). The reason to induce this unique orientation will be revealed in the XRD part later.

In fact, the orientation of ZnTPP is improved by increasing the 'evaporation time.' For example, the TCB-SC film (Figure 3e) has a slightly inferior molecular orientation than that of the TCB-DC film (Figure 3g) as found at the bands of 803 cm^{-1} on a fact that the drop-cast process needs a longer evaporation time than the spin-coating process. This suggests that a slower evaporation is preferable to a better crystallization, which would results in a better molecular orientation as revealed in the next section.

Analysis of Orientation Angle: Table 3 shows the orientation angles of the porphyrin and phenyl rings in the ZnTPP films revealed by pMAIRS using eq. (1), where ϕ_{por} and ϕ_{ph} are the angles of the 'plane normal' of the porphyrin and phenyl rings from the substrate normal, respectively (Figure 2). The angles of ϕ_{por} and ϕ_{ph}, are evaluated by using the $\gamma(C–H)_{por}$ band at about 800 cm^{-1} and the $\gamma(C–H)_{ph}$ band at about 700 cm^{-1}, respectively.

Table 3. The orientation angles of the porphyrin and phenyl rings. ϕ_{por} and ϕ_{ph} are the angles between the substrate normal and the direction of each vibration mode ($\gamma(C–H)_{por}$ and $\gamma(C–H)_{ph}$, respectively).

Film-preparation parameter	Porphyrin ring		Phenyl ring	
	ϕ_{por} / ° $\gamma(C–H)_{por}$	Orientation	ϕ_{ph} / ° $\gamma(C–H)_{ph}$	Orientation
Chl-SC	52	Random	59	Random
Chl-SC-A	31	Face-on	60	Random
Chl-DC	49	Random	51	Random
Chl-DC-A	39	Face-on	54	Random
TCB-SC	20	Face-on	70	Edge-on
TCB-SC-A	21	Face-on	73	Edge-on
TCB-DC	16	Face-on	73	Edge-on
TCB-DC-A	11	Face-on	78	Edge-on

As shown in Table 3, the orientation angles have a strong correlation with the evaporation time of the solvents. Note that, in the annealed TCB-DC film (denoted as "TCB-DC-A film") taking the longest time to evaporate the solvent, ϕ_{por} and ϕ_{ph} are 11° and 78°, respectively. The orientation angle of 11° is surprisingly small as compared even with the Langmuir monolayer on water (27° ± 3°)[43] and the vacuum vapor-deposited film (28° ± 10°).[19] The Chl-SC film, in contrast, exhibits a nearly isotropic structure. In fact, both orientation angles of the porphyrin and phenyl rings (52° and 59°, respectively) are fairly closed to the magic angle, 54.7°, which quantitatively confirms the isotropic structure. In a similar manner, other discussions in the previous sections have also been confirmed more quantitatively as found in Table 3.

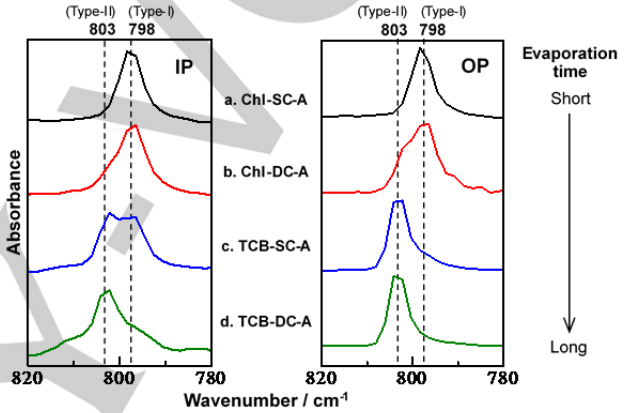

Figure 4. Magnified pMAIRS spectra of the $\gamma(CH)_{por}$ at ca. 800 cm^{-1} in the annealed ZnTPP thin films. The wavenumber positions of 798 and 803 cm^{-1} reflect to the type-I and -II crystals, respectively.

Influence of the evaporation time on the molecular arrangement revealed by IR spectroscopy: The molecular orientation of ZnTPP can thus be controlled by a combination of the solvent and film-preparation technique. Since both film-preparation parameters generally influence the crystallinity or the crystal structure of the final product, the crystallinity-sensitive IR band of the γ(C–H) mode is investigated.[44,45]

Figure 4 presents magnified pMAIRS spectra of the annealed ZnTPP thin films for the $\gamma(C–H)_{por}$ bands at about 800 cm^{-1}. The $\gamma(C–H)_{por}$ band is found to consist of two components corresponding to the used solvents: the Chl films have the band position at 798 cm^{-1} (Figures 4a and 4b); whereas the band appears at 803 cm^{-1} when the TCB solution is used (Figures 4c and 4d). As well as the $\gamma(C–H)_{por}$ band at ca. 800 cm^{-1}, the $\gamma(C–H)_{por}$ band at ca. 720 cm^{-1} also consists of the two components: the Chl films have the band position of 718 cm^{-1}; while the TCB films have that of 723 cm^{-1} (Figures 1 and 3). This implies that the ZnTPP films may comprise at least two different molecular arrangements reflecting different molecular interactions. At the moment, the two arrangements exhibiting the γ(C—H) bands at 798 and 803 cm^{-1} are named as type-I and type-II, respectively.

On closer inspection, the Chl-DC-A film (Figure 4b) contains not only the type-I, but also a minor type-II component in the OP spectra. In the case of the annealed TCB-SC film ("TCB-SC-A film"; Figure 4c), both types-I and -II are involved in the IP spectra. The intensity ratio of the two bands is correlated with

the solvent evaporation time: the relative intensity of the band at 803 cm^{-1} (correlated with type-II) to that at 798 cm^{-1} (type-I) becomes larger with an increase of the evaporation time (as summarized in Table 2). This trend is also found in the un-annealed films (Figure S1). Therefore, the 'molecular arrangement' of ZnTPP in the thin film is expected to be controlled by changing the evaporation time as confirmed in the next section.

Crystal structure analysis by XRD measurements: To support the IR results in Figure 4, the ZnTPP films were investigated by using GIXD. Figure 5 shows the GIXD patterns of annealed films in both IP and OP diffractions, and all the GIXD-IP patterns of the films are different from the GIXD-OP ones. This difference apparently indicates that ZnTPP crystallites are highly oriented in the thin films, as found in the IR results.

The crystal of ZnTPP is known to have polymorphism.[46-48] In fact, the GIXD patterns are of two different patterns marked by asterisks (*) and dots (●) as found in Figure 5. The Chl-SC-A film (Figure 5a) has an asterisk peak in both IP and OP patterns. On the other hand, the TCB-DC-A film (Figure 5d) exhibits totally different peaks marked by the dots with no asterisk peaks. The rest films (Figures 5b and 5c) consist of the two patterns. By referring to the calculated XRD patterns from the crystal structure reported in a previous study, the asterisk and dot peaks are readily assigned to the two different monoclinic crystal systems (CCDC Refcode: ZZZTAY03[46] and ZNTPOR03,[48] respectively). In this manner, the GIXD patterns apparently indicate that the ZnTPP films are of two polymorphs. Since the pattern variation perfectly agrees with those of the pMAIRS spectra (Figure 4), the former and latter monoclinic crystal systems should correspond to the molecular arrangements of type-I and -II, respectively. The IR bands at 798 and 803 cm^{-1} have thus been assigned to the two different molecular arrangements.

Figures 4 and 5 exhibit a good correlation that the type-I arrangement decreases while the type-II one increases with increasing the solvent evaporation time. This suggests that the type-I arrangement has a kinetically stable structure; while the type-II arrangement is thermodynamically favorable. According to Ruan et al.,[48] two nitrogen atoms of the porphyrin ring are coordinated with the hydrogen atoms of the neighboring phenyl rings in the monoclinic arrangement. Since type-II corresponds to the monoclinic arrangement, the edge-on orientation of the phenyl ring in the type-II films should be induced by the coordination, which also accounts for the thermodynamically stable character.

The evaporation time also influences the 'orientation of the crystallite' via the crystallinity change. As found in Figure 5b, the Chl-DC-A film comprises both types-I and -II with a major and minor quantities, respectively. Some of the type-II peaks (indexed by 110, 020 and 201) appear commonly in the GIXD-IP and -OP patterns. On the other hand, 'type-I' component has only 10-1 peak in the IP pattern, while it yields only 110 peak in the OP one. This implies that the major component, type-I, is highly oriented, while the coexisting type-II has a nearly random orientation.

In a similar manner, the TCB-SC-A film (Figure 5c) is analyzed to have a reversed conclusion that type-II is the major component with a highly oriented structure, while the minor type-I component has a random orientation. Thus, the crystal orientation of types-I and -II also has an apparent correlation with the evaporation time of the solvent.

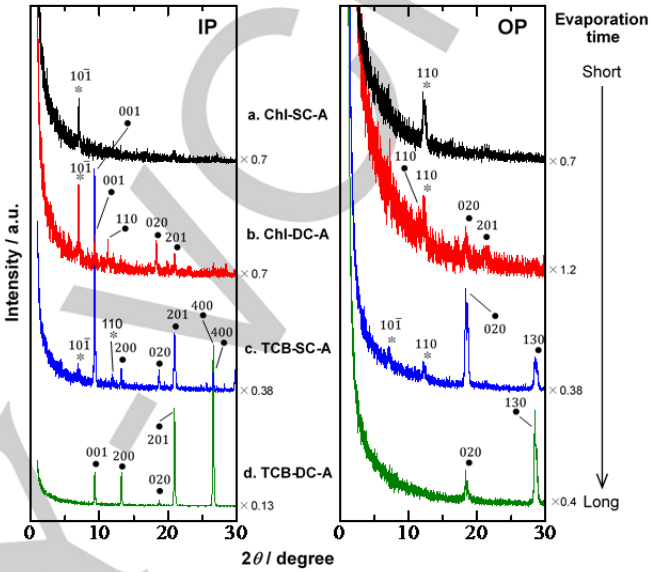

Figure 5. GIXD-IP and -OP patterns of the annealed ZnTPP thin films. The diffraction peaks marked with black circles and asterisks are assigned to the type-I and -II crystals, respectively.

Influence of thermal annealing studied by XRD measurements: Thermal annealing of a film is another important factor of molecular ordering. In the previous section, all the analyses were performed on annealed films. To investigate the annealing effect, un-annealed films are also analyzed.

Figure 6 shows the GIXD-IP and -OP patterns of the 'un-annealed' ZnTPP films. Of interest is that all the un-annealed films have no asterisk peak assigned to type-I; while the type-II peaks marked with dots appear. This means that the thermal annealing is necessary to generate the type-I 'crystal,' while the type-II crystal does not need annealing. This result looks strange when the IR results are taken into account. Since the un-annealed films of Chl-SC, Chl-DC and TCB-SC (Figure S1) exhibit the IR band at 798 cm^{-1} assigned to type-I arrangement, they should yield the asterisk peaks. This is because pMAIRS reveals 'molecular arrangement' in both amorphous and crystal; whereas GIXD responds to both molecular arrangement and the crystallinity, which is limited in a crystal. The 'molecular arrangement' such as the monoclinic crystal systems of type-I and -II in an un-annealed film is determined at the initial stage immediately after the solvent evaporation, but it has poor 'crystallinity.' Since pMAIRS is sensitive to the molecular arrangement irrespective of the crystallinity, the $\gamma(C–H)_{por}$ band appears apparently. After the thermal annealing, the molecular order is improved to have a good crystallinity, which gives GIXD peaks in type-I.

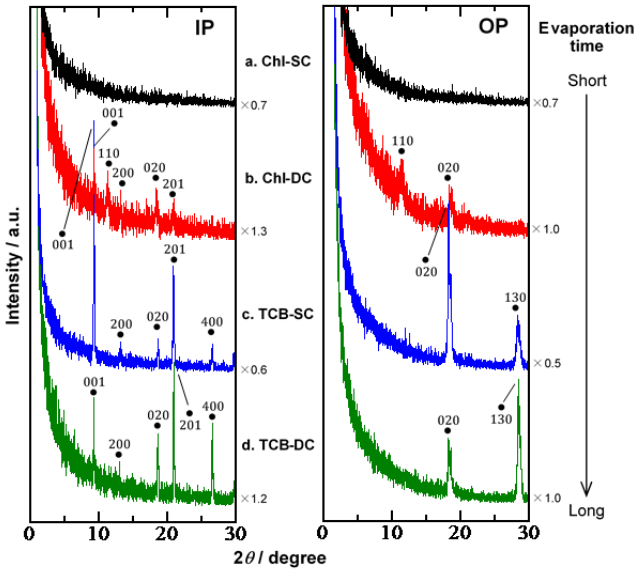

Figure 6. GIXD-IP and -OP patterns of the un-annealed ZnTPP thin films. The diffraction peaks marked with black circles and asterisks are assigned to the type-I and -II crystals, respectively.

In a similar manner, the type-II GIXD peaks of the annealed films are compared with those of the un-annealed ones (Figures 5 and 6). The annealed films apparently have stronger peaks than the un-annealed films, which confirms that crystallinity in type-II is improved by annealing the films.

As a conclusion, the effect of thermal annealing strongly depends on the initial state of molecular arrangement. Thus, the thermal annealing only helps improvement of the molecular order, and the solvent evaporation time is the dominant factor to determine the molecular arrangement of a ZnTPP film.

Conclusions

The molecular anisotropic structure of ZnTPP in films prepared by solution processes is comprehensively investigated by using a combinatorial technique of pMAIRS and GIXD. As a result, the molecular and crystal orientation, and the crystal structure are found to be controllable by the evaporation time of solvent depending on the two film-preparation parameters, a solvent and a film-preparation technique. The third parameter, thermal annealing, on the other hand, is found to mainly play a role for improving the crystallinity.

When a highly-volatile Chl solution is used for film-preparation, the porphyrin ring has the face-on orientation and this structure comes from the type-I arrangement; while in the TCB films taking the long time to become dried films, the type-II arrangement is generated where the porphyrin ring is highly oriented parallel to the substrate (11°), and the four phenyl rings on the porphyrin ring have a vertical stance (78°).

In addition, the component fraction and crystal orientation of types-I and -II are also correlated with the evaporation time. With increasing the evaporation time, the amounts of the type-I and -II crystallites are decreasing and increasing, respectively. In a similar manner, the crystal orientation of types-I and -II become inferior and improved, respectively, when a long evaporation time is taken. In this manner, the correlation between the molecular orientation and the crystal structure as a function of the film-preparation parameters is comprehensively revealed.

In the present study, because of the sublimation character of ZnTPP, the annealing was performed far below the melting point, which is a usual condition for small molecular compounds. In this case, the kinetically stable type-I arrangement keeps the arrangement, and it does not change into the thermodynamically stable type-II one. This confirms again that the molecular arrangement is not influenced by the annealing, but it is determined only by the solvent evaporation rate.

Experimental Section

Materials: Zinc(II) tetraphenylporphyrin (ZnTPP) was purchased from Tokyo Chemical Industry Co. Ltd. (Tokyo, Japan), which was used without further purification. Chloroform (Chl) was the ACS spectrophotometric grade with a purity of ≥ 99.8% and 1,2,4-trichlorobenezene (TCB) was the chromasolv® grade with a purity of ≥ 99%, which were both purchased from Sigma Aldrich (St. Louis, MO, USA).

Film Preparations: A Chl solution of ZnTPP with a volume of 20 μL at 10.0 mM was deposited on a silicon substrate using an Active (Saitama, Japan) ACT-300T Spincoater at 2000 rpm for 60 seconds to have a spin-coated (SC) film. In a similar manner, a TCB solution of 40 μL at 20.0 mM was used on the spin coater at 1000 rpm for a few seconds. The spinning time was changed depending on the character of the solvent. Since TCB has a weak affinity to the silicon substrate surface, for example, a spinning time was very short; otherwise most of the solvent would be thrown away. To have solvent-free films, several seconds and a few hours were spent, respectively, for the SC films made from the Chl and TCB solutions (abbreviated as “Chl-SC film” and “TCB-SC film,” respectively).

Drop-casted (DC) films were prepared by using a 2.0 mM Chl solution and a 4.0 mM TCB solution of ZnTPP (“Chl-DC film” and “TCB-DC film,” respectively). After spreading a solution with a volume of 40 μL on a silicon substrate, it was dried in ambient air for a minute and a few days, to evaporate Chl and TCB, respectively.

The thickness of the Chl-SC and -DC films were estimated by X-ray reflectivity measurements, and the SC and DC films were found to have the thickness of ca. 40 and 110 nm, respectively. All the films were prepared on a double-side polished silicon substrate with a square shape (40x20 mm^2) in ambient air (25°C), and the thermal annealing was performed at 100°C for 2 hours on an IKA (Osaka, Japan) C-MAG HS 4 hot-stirrer.

IR band assignment by DFT Calculations: Quantum-chemical calculations were performed by using the Gaussina09 program package.[49] The density functional theory (DFT) method was used with the B3LYP hybrid functional to calculate the molecular vibration frequencies and vibration modes. The 6-311+G(d,p) basis set[49] was used for Zn and the 6-311G(d,p) basis set[50] was used for the other atoms.

pMAIRS measurements: pMAIRS spectra in the wavenumber range from 4000 to 650 cm^{-1} were measured by using a Thermo Fischer Scientific (Madison, WI, USA) Nicolet 6700 FT-IR spectrometer equipped with a Thermo Fisher Scientific (Yokohama, Japan) automatic MAIRS equipment (TN10-1500). The p-polarized IR light was obtained by a Harrick Scientific (Pleasantville, NY, USA) PWG-U1R wire-grid polarizer. The transmitted light through the sample was detected by a liquid-N_2 cooled mercury-cadmium-telluride detector with a modulation frequency of 60 kHz. The angle of incidence was changed from 9° to 44° by 5° steps,[23,51] and the interferogram was accumulated 1000 times for each step.

The pMAIRS technique provides the in-plane (IP) and out-of-plane (OP) spectra simultaneously from an identical thin-film sample, which have the surface selection rule[52] corresponding to those of the conventional transmission and reflection absorption spectrometry, respectively. pMAIRS spectra have a great benefit that a quantitative analysis of the molecular orientation in a thin film can readily be carried out only by using the band intensity ratio between the IP and OP spectra[51] even with a rough surface.[37] Since the optical constants have already been taken into account in advance for choosing the optimal angles of incidence (9°-44°), the orientation angle of a transition moment, ϕ, is calculated by using eq. (1).[36,51,52]

$$\phi = \tan^{-1}\sqrt{\frac{2I_{\mathrm{IP}}}{I_{\mathrm{OP}}}} \qquad (1)$$

I_{IP} and I_{OP} are the peek intensities read from the IP and OP spectra, respectively. 1

GIXD measurements: GIXD measurements were performed by using a RIGAKU (Tokyo, Japan) SuperLab diffractometer with a Cu rotating anode X-ray generator operated at 40 kV and 30 mA (1.2 kW), generating the CuKα (λ = 0.15418 nm) radiation.[39] The XRD in-plane (IP) and out-of-plane (OP) patterns (denoted as GIXD-IP and -OP patterns) were obtained in the rage between $2\theta = 1°$ and 30° having a sampling step of 0.01° with a scan speed of 1° min^{-1}. For all the XRD measurements, the parallel X-ray beam was incident on the sample at the fixed angle of α = 0.20° from the surface parallel.

Acknowledgements

This work was financially supported by Grant-in-Aid for Scientific Research (A) (No. 15H02185 (TH)) and Grant-in-Aid for Young Scientists (B) (No. 26810075 (TS)) from Japan Society for the Promotion of Science, for which the authors thanks are due.

Keywords: pMAIRS • GIXD • molecular orientation • thin films • porphyrinoids

[1] J. Wu, H. A. Becerril, Z. Bao, Z. Liu, Y. Chen, P. Peumans, *Appl. Phys. Lett.* **2008**, 92, 263302.
[2] T. Shimoda, Y. Matsuki, M. Furusawa, T. Aoki, I. Yudasaka, H. Tanaka, H. Iwasawa, D. Wang, M. Miyasaka, Y. Takeuchi, *Nature* **2006**, *440*, 783-786.
[3] P. Calvert, *Chem. Mater.* **2001**, *13*, 3299-3305.
[4] H. Sirringhaus, T. Kawase, R. H. Friend, T. Shimoda, M. Inbasekaran, W. Wu, E. P. Woo, *Science* **2000**, *290*, 2123-2126.
[5] M. Singh, H. M. Haverinen, P. Dhagat, G. E. Jabbour, *Adv. Mater.* **2010**, *22*, 673-685.
[6] A. R. Ingo, H. C. Chiu, W. Fann, Y. S. Huang, U. S. Jeng, C. H. Hsu, K. Peng, S. Chen, *Synth. Met.* **2003**, *139*, 581-584.
[7] C. D. Dimitrakopoulos, P. R. L. Malenfant, *Adv. Mater.* **2002**, *14*, 99-117.
[8] U. Zschieschang, F. Ante, D. Kälblein, T. Yamamoto, K. Takimiya, H. Kuwabara, M. Ikeda, T. Sekitani, T. Someya, J. Blochwitz-Nimoth, H. Klauk, *Org. Electron.* **2011**, *12*, 1370-1375.
[9] M. K. Debe, K. K. Kam, J. C. Liu, R. J. Poirier, *J. Vac. Sci. Technol. A* **1988**, 1907-1911.
[10] A. Koma, *Prog. Cryst. Growth Charact. Mater.* **1995**, *30*, 129-152.
[11] K. Walzer, T. Toccoli, A. Pallaoro, S. Lannotta, C. Wagner, T. Fritz, K. Leo, *Surf. Sci.* **2006**, *600*, 2064-2069.
[12] M. Hara, H. Sasabe, A. Yamada, A. F. Garito, *Jpn. J. Appl. Phys.* **1989**, *28*, L306.
[13] J. E. Anthony, J. S. Brooks, D. L. Eaton, S. R. Parkin, *J. Am. Chem. Soc.* **2001**, *123*, 9482-9483.
[14] M. M. Payne, S. R. Parkin, J. E. Anthony, C. C. Kuo, T. N. Jackson, *J. Am. Chem. Soc.* **2005**, *127*, 4986-4987.
[15] K. Takimiya, H. Ebata, K. Sakamoto, T. Izawa, T. Otsubo, Y. Kunugi, *J. Am. Chem. Soc.* **2006**, *128*, 12604-12605.
[16] H. Ebata, T. Izawa, E. Miyazaki, K. Takimiya, M. Ikeda, H. Kuwabara, T. Yui, *J. Am. Chem. Soc.* **2007**, *129*, 15732-15733.
[17] R. Hofmockel, U. Zschieschang, U. Kraft, R. Rödel, N. H. Hansen, M. Stolte, F. Würthner, K. Takimiya, K. Kern, J. Pflaum, H. Klauk, *Org. Electron.* **2013**, *14*, 3213-3221.
[18] M. G. Walter, A. B. Rundine, C. C. Wamser, *J. Porphyrins Phthalocyanines* **2010**, *14*, 759-792.
[19] S. Narioka, H. Ishii, Y. Ouchi, T. Yokoyama, T. Ohta, K. Seki, *J. Phys. Chem.* **1995**, *99*, 1332-1337.
[20] J. Cai, H. Chen, J. Huang, J. Wang, D. Tian, H. Dong, L. Jiang, *Soft Matter* **2014**, *10*, 2612-2618.
[21] J. Spadavecchia, R. Rella, P. Siciliano, M. G. Manera, A. Alimelli, R. Paolesse, C. D. Natale, A. D'Amico, *Sensors and Actuators B* **2006**, *115*, 12-16.
[22] T. Nonaka, Y. Mori, N. Nagai, T. Matsunobe, Y. Nakagawa, M. Saeda, T. Takahagi, A. Ishitani, *J. Appl. Phys.* **1993**, *73*, 2826-2830.
[23] N. Shioya, T. Shimoaka, K. Eda, T. Hasegawa, *Phys. Chem. Chem. Phys.* **2015**, *17*, 13472-13479.
[24] H. Sirringhaus, P. J. Brown, R. H. Friend, M. M. Nielsen, K. Bechgaard, B. M. W. Langeveld-Voss, A. J. H. Spiering, R. A. J. Janssen, E. W. Meijer, P. Herwing, D. M. De Leeuw, *Nature* **1999**, *401*, 685-688.
[25] B. O'Connor, R. J. Kline, B. R. Conard, L. J. Richter, D. Cundlach, M. F. Toney, D. M. DeLongchamp, *Adv. Funct. Mater.* **2011**, *21*, 3697-3705.
[26] M. L. Swiggers, G. Xia, J. D. Slinker, A. A. Gorodetsky, G. G. Malliaras, R. L. Headrick, B. T. Weslowski, R. N. Shashidhar, C. S. Dulcey, *Appl. Phys. Lett.* **2001**, *79*, 1300-1302.
[27] C. D. Dimitrakopoulos, A. R. Brown, A. Pomp, *J. Appl. Phys.* **1996**, *80*, 2501-2508.
[28] J. F. Chang, B. Sun, D. W. Breiby, M. M. Nielsen, T. I. Sölling, M. Giles, I. McClloch, H. Sirringhaus, *Chem. Mater.* **2004**, *16*, 4772-4776.
[29] N. Shioya, T. Shimoaka, T. Hasegawa, *Chem. Lett.* **2014**, *43*, 1198-1200.
[30] X. H. Kong, K. Deng, Y. L. Yang, Q. D. Zeng, C. Wang, *J. Phys. Chem. C* **2007**, *111*, 9235-9239.
[31] G. Li, V. Shrotriya, J. Huang, Y. Yao, T. Moriarty, K. Emery, Y. Yang, *Nat. Mater.* **2005**, *4*, 864-868.
[32] C. M. Che, H. F. Xiang, S. S. Y. Chui, Z. X. Xu, V. A. L. Roy, J. J. Yan, W. F. Fu, P. T. Lai, I. D. Williams, *Chem. Asian J.* **2008**, *3*, 1092-1103.
[33] T. Hasegawa, *Anal. Chem.* **2007**, *79*, 4385-4389.
[34] T. Hasegawa, Y. Itoh, A. Kasuya, *Anal. Sci.* **2008**, *24*, 105-109.
[35] Y. Itoh, A. Kasuya, T. Hasegawa, *J. Phys. Chem. A* **2009**, *113*, 7810-7817.
[36] T. Hasegawa, *Appl. Spectrosc. Rev.* **2008**, *43*, 181-201.
[37] Drapcho, D.; Hasegawa, T. *Spectroscopy* (Special Issue), **2015**, *30*, 31-38.
[38] K. Omote, J. Harada, *Adv. X-ray Anal.* **2000**, *43*, 192-200.

[39] K. Omote, *J. Phys.: Cond. Mat.* **2010**, *22*, 474004.
[40] T. N. Lomova, B. D. Berezin, *Russ. J. Coord. Chem.* **2001**, *27*, 85-104.
[41] J. O. Alben, S. S. Choi, A. D. Adler, W. S. Caughey, *Ann. N.Y. Acad. Sci.* **1973**, *206*, 278-295.
[42] H. Ogoshi, Y. Saito, K. Nakamoto, *J. Chem. Phys.* **1972**, *57*, 4194-4202.
[43] H. Nagatani, H. Tanida, T. Ozeki, I. Watanabe, *Langmuir* **2006**, *22*, 209-212.
[44] Y. Yuan, J. Zhang, J. Sun, J. Hu, T. Zhang, Y. Duan, *Macromolecules* **2011**, *44*, 9341-9350.
[45] K. Yazawa, Y. Inoue, T. Yamamoto, N. Asakawa, *J. Phys. Chem. B* **2008**, *112*, 11580-11585.
[46] M. P. Byrn, C. J. Curtis, I. Goldberg, Y. Hsiou, S. I. Khan, P. A. Sawin, K. Tendick, C. E. Strouse, *J. Am. Chem. Soc.* **1991**. *113*, 6549-6557.
[47] W. R. Scheidt, J. U. Mondal, C. W. Eigenbrot, A. Adler, L. J. Randonovich, J. L. Hoard, *Inorg. Chem*. **1986**. *25*, 795-799.
[48] W. J. Ruan, Z. A. Zhu, X. H. Bu, Z. H. Zhang, Y. Shao, Y. T. Chen, *Chin. J. Struct. Chem.* **1998**, *17*, 159-164. ZnTPP in the monoclinic single crystal reported in this paper is a monohydrate. ZnTPP of type-II in our thin films, however, is not hydrated (see the $\delta(H_2O)$ region around 1650 cm^{-1} in Figure 3). This suggests that the hydration is not important to have the type-II crystallites.
[49] M. J. Frisch, et al. *GAUSSIAN 09*, revision D.01; Gaussian, Inc.: Waillingford, CT, 2009.
[50] R. C. Binning, L. A. Curtiss, *Comp. Chem.* **1990**, *11*, 1206-1216.
[51] N. Shioya, S. Norimoto, N. Izumi, M. Hada, T. Shimoaka, T. Hasegawa, *Appl. Spectrosc.* **2016**, *70*, in press.
[52] T. Hasegawa, *J. Phys. Chem. B* **2002**, *106*, 4112-4115.

Entry for the Table of Contents (Please choose one layout)

Layout 1:

FULL PAPER

Text for Table of Contents

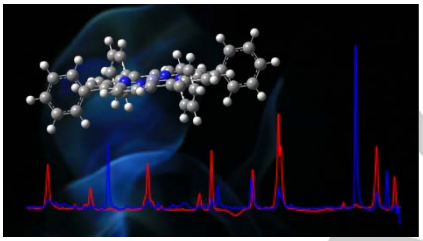

*M. Hada, N. Shioya, T. Shimoaka, K. Eda, M. Hada, T. Hasegawa**

Page No. 1 – 8

Comprehensive Understanding of Structure-Controlling Factors of a Zinc Tetraphenylporphyrin Thin Film Studied by pMAIRS and GIXD Technique.